NQO1-responsive Prodrug for *in Cellulo* Release of Cytochalasin B as Cancer Cell-targeted Migrastatic

Mervic D. Kagho,[a,#] Katharina Schmidt,[b,#] Christopher Lambert,[c,d] Lili Jia,[d] Klemens Rottner,[c] Marc Stadler,[d] Theresia Stradal,*[,b] and Philipp Klahn*[,a]

[a] Dr. Mervic D. Kagho, Prof. Dr. P. Klahn
Department of Chemistry and Molecular Biology, Division of Organic and Medicinal Chemistry
University of Gothenburg
Natrium, Medicinaregatan 7B, 413 90 Gothenburg, Sweden
E-mail: philipp.klahn@gu.se

[b] K. Schmidt, Prof. Dr. T. Stradal
Department of Cell Biology
Helmholtz Centre for Infection Research
Inhoffenstrasse 7, D-38124 Braunschweig, Germany
E-mail: theresia.stradal@helmholtz-hzi.de

[c] C. Lambert, Prof. Dr. K. Rottner
Department of Molecular Cell Biology
Helmholtz Centre for Infection Research
Inhoffenstrasse 7, D-38124 Braunschweig, Germany

[d] C. Lambert, L. Jia, Prof. Dr. M. Stadler
Department of Microbial Drugs
Helmholtz Centre for Infection Research
Inhoffenstrasse 7, D-38124 Braunschweig, Germany

# Authors contributed equally.

Supporting information for this article is given via a link at the end of the document.

Abstract: Migrastatic drugs targeting cell motility and thereby suppress invasiveness of solid cancer cells, including their ability to metastasize and establish secondary tumors, are of high interest and have the potential to bring about a paradigm shift in the treatment of solid cancer. Cytochalasans, such as cytochalasin B, are known to disrupt cytoskeletal dynamics by inhibiting actin polymerization and have attracted considerable attention as potential migrastatics over the last decades, but are limited by selectivity issues so far. We herein report on the design, synthesis and evaluation of a bioresponsive prodrug **BQTML-CB** cleavable by the quinone-oxidoreductase NQO1, discussed as therapeutic target for the treatment of cancer.

Introduction

Cancer remains one of the leading causes of death and a significant global burden with over 10 million deaths worldwide annually.[1] In contrast to hematologic malignancies (involving the blood, bone marrow and lymphatic system), predominantly characterized by uncontrolled clonal proliferation,[2,3] cells associated with solid tumors may invade the surrounding tissue and spread to other body parts (metastasis). This is believed to account for more than 90% of the observed mortality.[4,5] Conventional cytostatic anticancer therapies, on the other hand, primarily target cell proliferation, which makes up for the majority of treatment options currently available.[6]

In 2017 *Gandalovičová et al.* proposed the term “migrastatics” for anticancer drugs interfering with all modes of cancer cell invasiveness, including their ability to overcome the extracellular matrix (ECM) and establish secondary tumors.[6] An anticancer therapy aiming towards migrastasis may potentially pose a paradigm change in solid cancer treatment[7], as anti-metastatic agents[8] show synergistic effects with conventional therapies based on antiproliferation and cytotoxic effects[9,10]. It was proposed that the selection pressure exerted by such agents may not cause resistance towards conventional therapies because the mechanisms targeted are of complete different nature.[7,11]

Potential targets for migrastatic anticancer therapies are those directly or indirectly associated with cell motility, such as availability of ATP, mitochondrial metabolism, cytoskeletal dynamics, cell adhesion, cell polarization, ECM remodeling pathways and cell contractility.[11,12] Actin plays a crucial role in most if not all motile processes of eukaryotic cells, including changes of cell shape, cell migration, vesicular trafficking, and cytokinesis.[13]

In this context, natural compounds interfering with actin polymerization and contractility, such as cytochalasans, jasplakinolide, latrunculins, staurosporine and scytophycins have attracted particular research interest as potential migrastatics.[8,9,12]

Cytochalasans[14] are a large family of fungal secondary metabolites produced by many members across the Ascomycota, such as *Diaporthe* and *Chaetomium*.[15,16] Cytochalasans are biosynthesized in concerted action of a fungal polyketide synthase and a non-ribosomal peptide synthetases (PKS-NRPS)[17] commonly comprising a tricyclic structure consisting of an isoindolone core fused to a macrocyclic ring.[18,19] The

structurally diverse family of cytochalasans displays a broad range of interesting biological activities,[20–22] but the most prominent activity of cytochalasans encountered in all cytochalasan sub-classes is their inhibition of actin polymerization and/or disruption of actin filaments.[21,22]

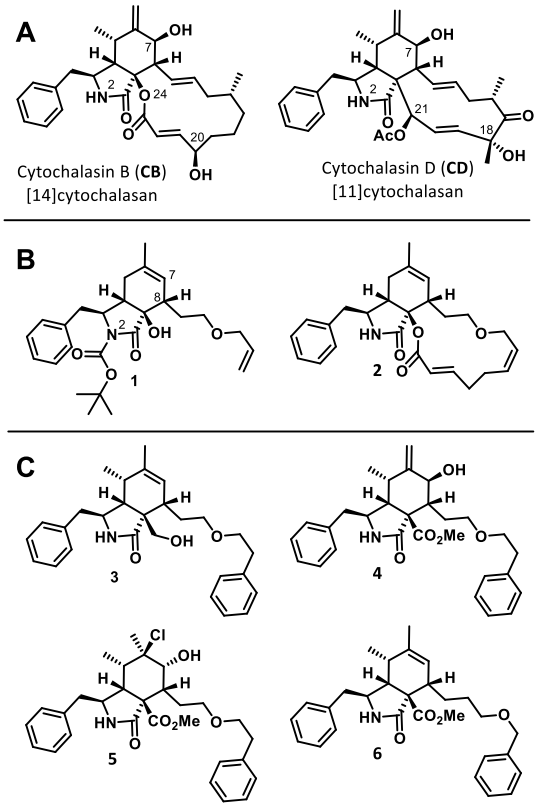

Figure 1. (**A**) Structures of cytochalasin B (**CB**) and cytochalasin D (**CD**). (**B**) cytochalasin B-inspired analogues by *Waldmann* and co-workers.[23] (**C**) Cytochalasan analogues lacking the macrocyclic moiety reported by *Perlíková* and co-workers.[24] Atom numbering follows the nomenclature for cytochalasans introduced by *Binder et al.*.[25]

Cytochalasans were shown to exhibit strong cytotoxic and antiproliferative activities against murine and human cancer cell lines[17,18,22,26], conceivably linked to their bioactivity against actin, generally considered as a limiting factor impeding their applicability.

Nevertheless, cytochalasin D (**CD**), a representative of the [11]cytochalasan subclass and cytochalasin B (**CB**), a representative of the [14]cytochalasan sub class (Figure 1) have been studied for their anticancer activities early on. Their efficacy was investigated *in vitro* and *in vivo*,[26–31] with most studies focusing on **CB**, as it appears to be 20-fold less toxic than **CD** to mice.[31,32] Additionally and in contrast to **CD**, **CB** inhibits GLUT transporters[33] and potentially prevents glycolysis.[34–37] Glucose transporters have drawn a lot of interest as chemotherapeutic agents because most cancer cells rely primarily on high rates of glycolysis to maintain metabolic activity instead of relying on the potential for pyruvate oxidation in mitochondria to induce oxidative phosphorylation.[9,38] Thus, **CB** combines two favorable anticancer mechanisms. Finally yet importantly, in 2015 *Trendowski et al.* demonstrated synergistic potentiation of the microtubule binder paclitaxel and the topoisomerase inhibitor doxorubicin by **CB** in human ovarian carcinoma SKVLB1[10] as well as synergistic effects *in vitro* and *in vivo* in multi-drug resistant murine P388/ADR leukemia.[31]

The key challenge for the design of cytochalasin B based migrastatics is the reduction of systemic toxicity and improvement of selectivity for cancer cells. In 2015, *Waldmann* and co-workers demonstrated in a *de novo* synthesis approach of **CB**-inspired simplified analogues that actin disruption and cytotoxic effects can be conceptually decoupled.[23] The CB-analogues **1** and **2** (Figure 1B) resembled the characteristic architecture of the natural product at the scaffold level, yet were glucose import inhibitors only, not showing any actin binding. Recently, *Perlíková* and co-workers published CB-derived synthetic cytochalasan analogues **3**-**6** (Figure 1C) lacking the macrocyclic moiety but bearing aryl containing side chains in the C10 position, which showed significantly reduced cytotoxicity against human BLM melanoma cells (at least 2-fold) and human MRC-5 fibroblasts (at least 185-fold) compared to **CB**.[24] The reported compounds retained some, although only modest, bioactivity in an actin polymerization assay *in vitro* and the actin network of living cells and exerted migrastatic activity in a spheroid invasion assay with BLM cells. Whether their compounds inhibit glucose import was not tested.

Although their results indicate that migrastatic and antiproliferative activities can be uncoupled – which offers promising prospects for further development of cytochalasin-analogues as migrastatics – the drastic reduction of migrastatic activity of these compounds might limit their potential currently.

However, we need to consider that targeting actin cytoskeleton dynamics and/or contractility affects many processes in both cancer and non-cancer cells, such as cell migration, division, and exocytosis. Additionally, it has been shown that systemic administration of CB induces immunosuppression in *in vivo* murine tumor models,[30] potentially affecting immune processes by interfering with both mesenchymal and amoeboid migration of leukocytes. Thus, migrastatic effects need to be confined and selective for tumors, which seems to be even more important than the reduction of specific antiproliferative activity.

Here, we report the design, synthesis, *in vitro* and cell biological evaluation of the semi-synthetically accessed, bioresponsive prodrug **BQTML-CB** (Scheme 1) to turn the migrastatic activity of **CB** towards cancer cells over-expressing the quinone-oxidoreductase NQO1 to increase cancer cell selectivity.

Results and Discussion

SAR and design of BQTML-CB

Cytochalasans such as **CB**[39–41] as well as numerous other cytochalasans[18,42,43,43–57] have been targeted by elegant total synthesis campaigns for more than 40 years[18,19,58–60].

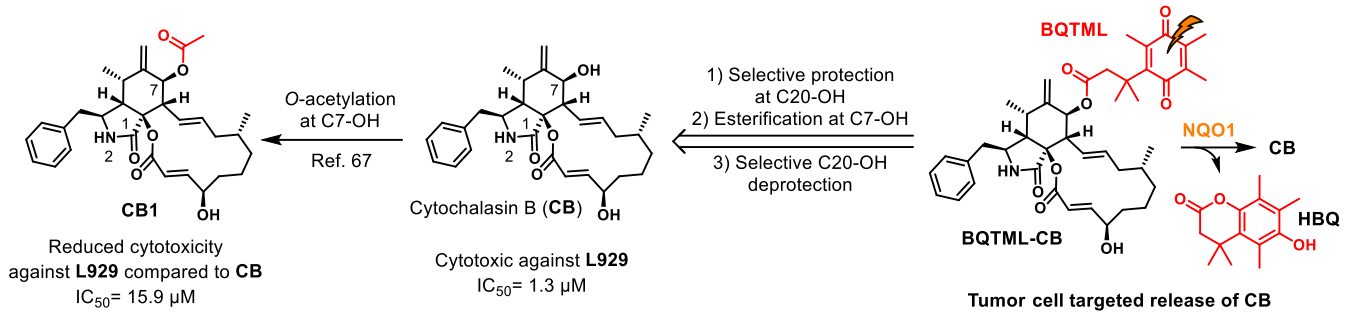

Scheme 1. Structures of cytochalasin B (**CB**) and its derivative **CB1** and **BQTML-CB**.

However, so far, total synthesis routes are lengthy and expensive in terms of time and low overall yield[61] failing to supply sufficient amounts of cytochalasans for derivatization campaigns. Even the synthesis of the structurally simplified CB analogues **3**-**6** (Figure 1C) requires at least 10-13 steps from commercially available starting materials and proceeds in overall yields between 1-2%.[24] In contrast, availability has improved in recent years due to mass production via exploitation of fungal producers,[62,63] establishment of mutasynthesis approaches[64] and PKS-NRPS engineering[65] of certain cytochalasan-producing biosynthetic gene clusters. **CB** can be obtained in sufficient amounts in batch fermentations using submerged cultures in shaking flasks of the endophytic fungus *Preussia Similis* G22 (DSM32328) as described by *Kretz et al.*.[21,66]. This allows for the exploration of semi-synthetic modifications of **CB**.

Within our recent work,[66] we shed light on the structure-activity relationship of **CB** on actin by virtual docking and semi-synthetic modification. We found that **CB** occupies the same binding pocket *in silico* as **CD** when docked onto non-polymerizable monomeric G-actin (PDB: 3EKU)[67], although binding less tightly to actin as the larger macrocycle of the [14]cytochalasin **CB** does not allow to penetrate as deep as **CD** into the binding pocket, resulting in a reduced hydrogen bridge network for **CB**. We furthermore determined the importance of the C7-OH function of **CB** for its actin binding activity and were able to show that **CB1** (Figure 1), a semi-synthetic derivative of **CB**, obtained by *O*-acetylation of the hydroxyl group at C7-OH position of the 6-membered ring, exhibited a significantly reduced cytotoxic activity against mouse connective tissue fibroblasts L929 with an IC_{50} value of 15.9 µM versus 1.3 µM for **CB**. In addition, a high dose treatment of the filamentous actin (F-actin) network of human osteosarcoma cells (U-2OS) with **CB1** showed no impact on the actin filaments in contrast to the high dose treatment with **CB** leading to the collapse of the entire F-actin network, indicating the importance of this moiety for actin interaction.[66]

Identifying the same binding pocket for **CD** and **CB**,[66] we hypothesized that the attachment of larger groups in the C7-OH position would further reduce both, cytotoxic as well as migrastatic activity, similar to photoactivatable probes of **Nvoc-CD** (structure not shown) published earlier by *Nair et al.*.[68]

In order to confine **CB**'s migrastatic and cytotoxic properties to tumor cells, we envisaged to introduce a bulky benzoquinone Trimethyl-Lock (BQTML)[69] ester responsive to the tumor-associated enzyme NQO1 to the C7-OH position of **CB**.[70] Thus, in the resulting **BQTML-CB** (Scheme 1) the C7-OH would be masked, reducing actin binding and cytotoxicity significantly, while upon tumor-associated presence of NQO1 the reductive, autoimmolative release of **CB** (and the corresponding BQTML-derived hydrobenzoquinone **HBQ,** Scheme 1) is envisaged unfolding its migrastatic and cytotoxic activity in selective manner. BQTML esters are known to be serum stable due to their high steric hindrance of the three pendant methyl groups and have been extensively used in the development of chemical probes that target NQO1.[69]

The flavin-containing quinone reductase NQO1 (NAD(P)H quinone oxidoreductase 1) is found in almost all mammals. It catalyzes the two-electron reduction of quinones into hydroquinones by using either NADPH or NADH as electron donors and FMN as prosthetic group.[71,72] NQO1 is constitutively expressed at relatively low levels in a variety of healthy tissues under physiological conditions, with over 90% localized in the cytosol.[71] It has been shown that expression of NQO1 is highly up-regulated in solid tumors such as cholangiocarcinoma, breast, cervical, and lung cancers, and that elevated levels of NQO1 are associated with cancer progression, metastasis[73,74] and bad prognosis for the patients.[71,72] Consequently, NQO1 has received a lot of attention as biomarker for cancer imaging and therapy.[72]

Semi-synthesis of BQTML-CB

To prove our concept we aimed to semi-synthesize the antimetastatic prodrug **BQTML-CB** starting from **CB** obtained by fermentation of *Preussia simillis* G22 (DSM 32328) as described by *Kretz et al.*.[21,66] Therefore, BQTML carboxylic acid **7** was accessed *via* a two-step sequence (Scheme 2) following a slightly modified procedure earlier described by *Rohde et al.*.[75]

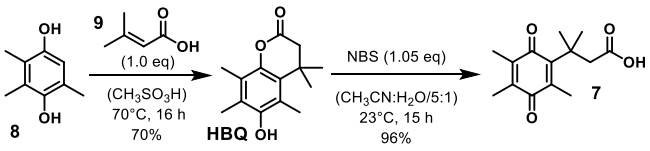

Scheme 2. Synthesis of the BQTML carboxylic acid **7**.

First, a *Friedel–Crafts* type condensation of commercially available 2,3,5-trimethyl-1,4-benzenediol (**8**) with 3-methyl-2-butenoic acid methyl ester (**9**) in methanesulfonic acid at 70°C furnished the hydrobenzoquinone **HBQTML** in 70% yield. Subsequent oxidation with *N*-bromosuccinimide at 23°C gave BQTML carboxylic acid **7** in 96% yield.

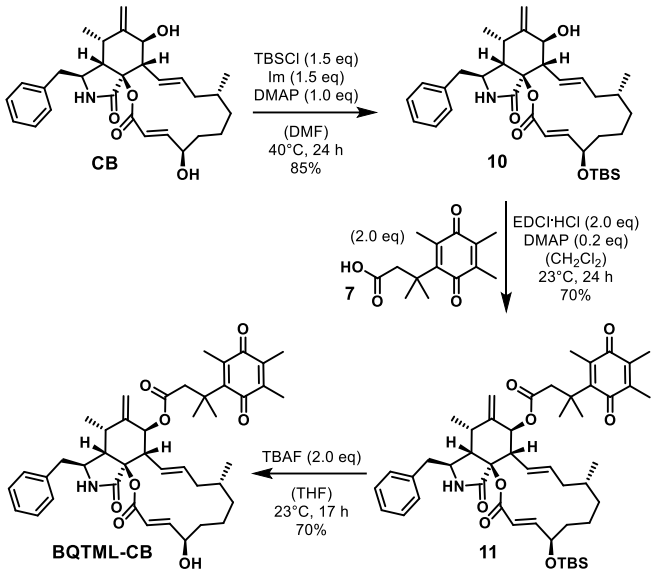

Scheme 3. Semi-synthesis of **BQTML-CB**.

In parallel, as described earlier by us,[66] the treatment of **CB** with TBSCl in the presence of imidazole and DMAP at 40°C, resulted in a selective *O*-silylation of the C20-OH group to afford compound **10** in 85% yield (Scheme 3). Compound **7** was activated with EDCI·HCl in the presence of a stoichiometric amount of DMAP and imidazole in anhydrous CH_2Cl_2 for 30 min and coupled to the C7-OH forming BQTML-ester **11** in 70% yield. Finally, the desired **BQTML-CB** was accessed by cleaving the C20-OTBS group with a 1 M-solution of TBAF in 70 % yield as outlined in Scheme 3.

In vitro NQO1 activation of BQTML-CB

With the prodrug **BQTML-CB** in hand, we next investigated the release of **CB** in the presence of commercially available human NQO1 recombinantly expressed in *E. coli* by LC-MS analysis. Therefore, **BQTML-CB** was incubated with NQO1 in the presence of required co-factors NADH and FMN in TRIS buffer (20 mM, pH 7.4) at 37°C and after removal of the enzyme by 10 kDa cut-off spin columns we analyzed the solution by LC-MS (Figure 2). **BQTML-CB** (Figure 2 B1: R_t = 5.15 min and C1: mass 710 m/z for $[M-H]^-$) was completely converted into **CB** (Figure 2 B4: R_t = 3.71 min and C2: mass 480 m/z for $[M-H]^+$) and **HBQ** (Figure 2 B4: R_t = 3.51 min and C3: mass 235 m/z for $[M-H]^+$) within 10 min at 37°C. No intermediate **HBQTML-CB** (Figure 2 A) was observed. The conversion was depending on the presence of NQO1 as well as the co-factors NADH and FMN. In absence of either of them no conversion was observed.

In cellulo activation of BQTML-CB to release CB

Next, we initially screened for **BQTML-CB** responding and non-responding cell lines. Four standard wild type cell lines were tested, namely human osteosarcoma cells (U-2OS), mouse melanoma cells (B16-F1), mouse fibroblasts (NIH 3T3), and rat fibroblasts (Rat2) in a 24 h proliferation assay.

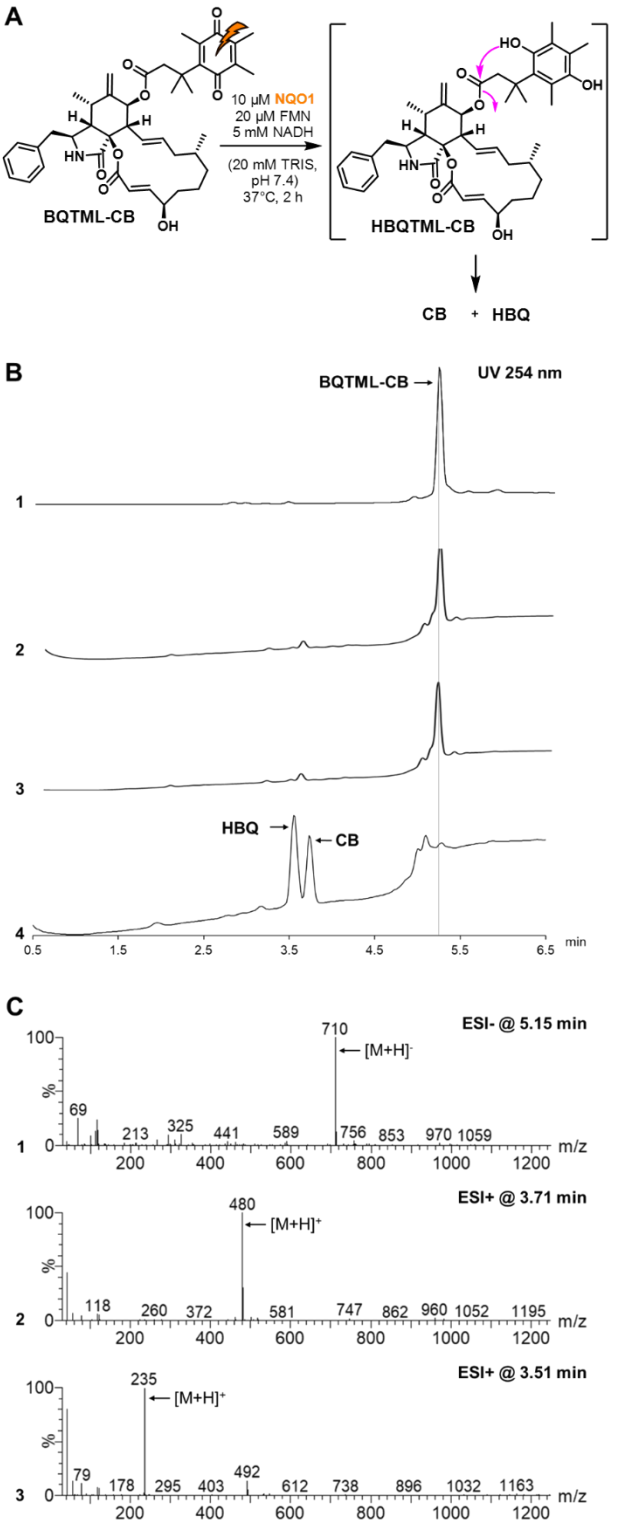

Figure 2. (**A**): Mechanism of NQO1-mediated release of **CB** and **HBQ**. (**B**): UV chromatogram at 254 nm of (**B1**): **BQTML-CB** (500 µM) in TRIS buffer (20 mM, pH 7.4), (**B2**): **BQTML-CB** (500 µM) after 10 min incubation with FMN (20 µM) and NADH (5 mM) in TRIS buffer (20mM, pH 7.4) at 37°C. (**B3**): **BQTML-CB** (500 µM) after 10 min incubation with human NQO1 (10 µM) in TRIS buffer (20mM, pH 7.4) at 37°C. (**B4**): **BQTML-CB** (500 µM) after 10 min incubation with human NQO1 (10 µM), FMN (20 µM), NADH (5 mM) in TRIS buffer (20mM, pH 7.4) at 37°C. (**C**): ESI^- or ESI^+ mass spectra of (**C1**): **B1** @5.15 min, (**C2**): **B4** @4.72 min, and (**C3**): **B4** @3.51 min.

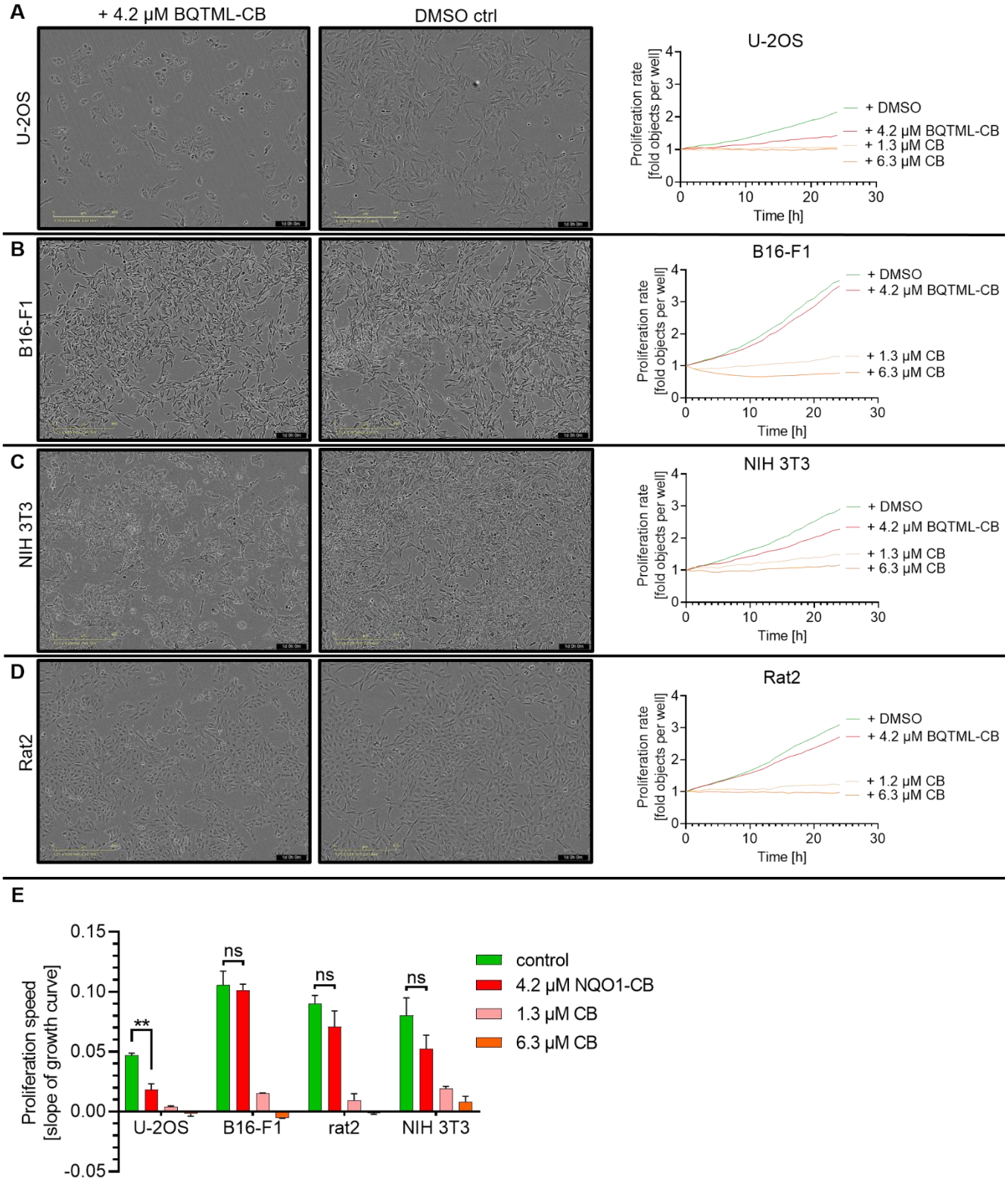

Figure 4. Analysis of cell proliferation during 24 h BQTML-CB treatment. Phase contrast images of U-2OS (**A**), B16-F1 (**B**), NIH 3T3 (**C**), and rat2 (**D**) recorded after 24 h treatment with 4.2 µM BQTML-CB and DMSO as vehicle control. The proliferation rate was assessed by automated cell count for 24 h and plotting the mean phase object counts from at least two independent experiments with two replicates against the time. (**E**) Normalized proliferation speed was determined by calculating the slope from the growth curves between 0 and 24 hours. Data are means + SEM; n = 2, ** p<0.0014, ordinary one-way ANOVA

Here, cell lines were treated with 4.2 µM **BQTML-CB** – referring to the previous determined IC_{50} concentration of **CB**[66] - and DMSO as vehicle control. Proliferation was analysed using the IncuCyte S3 Adherent Cell-by-Cell module of its Live Cell Analysis Software (Figure 4). A commercial **CB** standard was utilized in low (1.25 µM) and high (6.25 µM) concentrations, enabling the comparison of bioactivity of released and activated **CB**. Significantly reduced proliferation of U-2OS cells after **BQTML-CB** treatment, similar to low dose concentrations of CB was observed (Figure 4A and E), whereas **BQTML-CB** treated B16-F1 cells were nearly unaffected (Figure 4B and E). In contrast, NIH 3T3 and Rat2 cells by trend, but not in statistically significant fashion showed impaired proliferation (Figure 4C, D, and E). In addition, morphological alterations like flattening, rounding and cell grouping were noted for U-2OS and NIH 3T3 after 24 h **BQTML-CB** treatment (Figure 4A and C; see representative phase contrast images). As cell grouping is a common indicator for diminished cell motility and since **CB** is well-known and utilized as a versatile actin inhibitor, we wondered if these effects are due to changes in the actin architecture.

Impact of BQTML-CB on F-actin network

To investigate possible consequences of **BQTML-CB** treatment on cellular level, we stained F-actin and nuclear DNA after 24 h of **BQTML-CB** (4.2 µM) treatment. **CB** in low (1.3 µM) and high (6.3 µM) concentrations served as comparative controls.

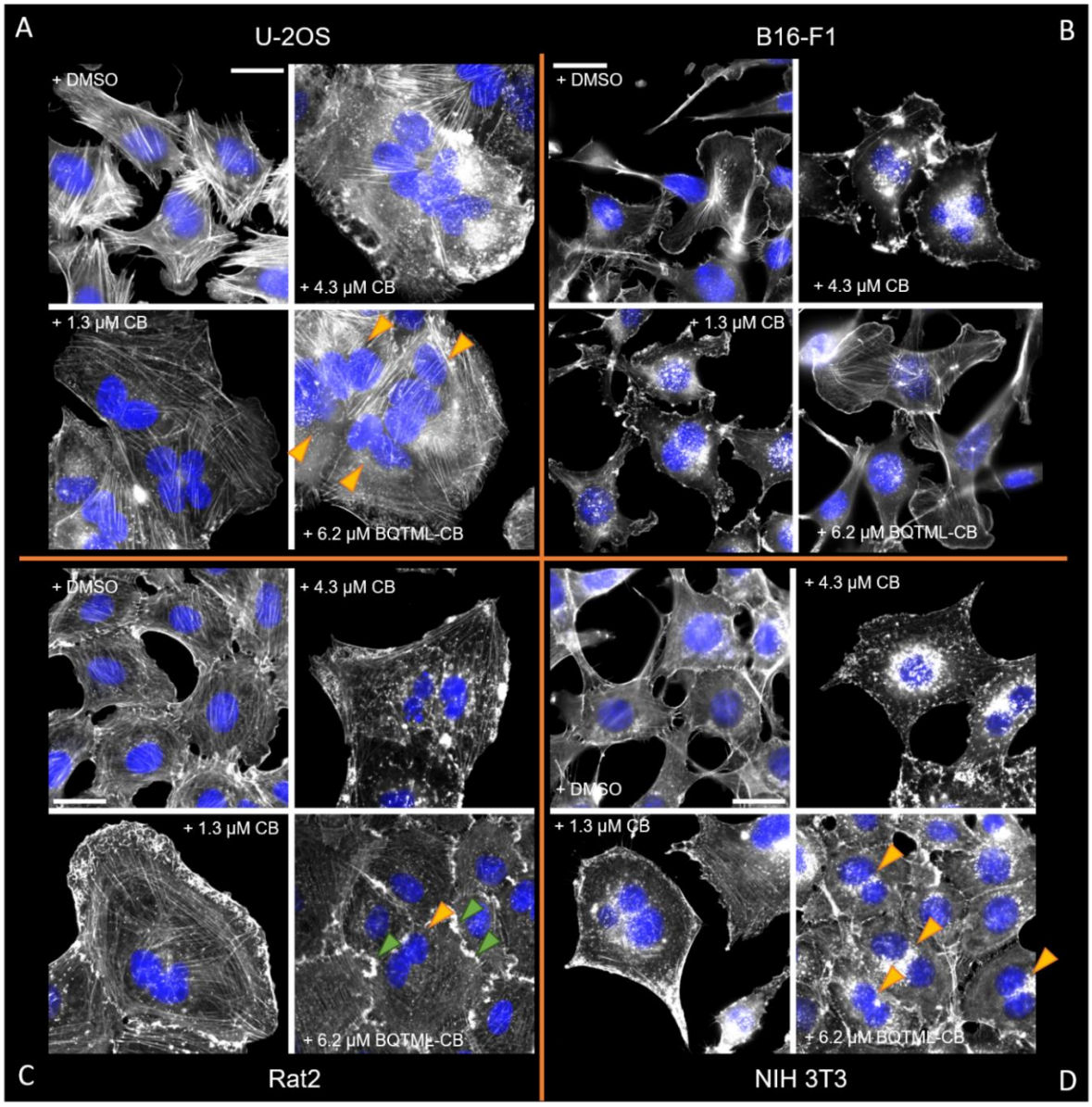

Figure 5. Overlay images of **CB**, **BQTML-CB** and DMSO treated U-2OS (**A**), B16-F1 (**B**), Rat2 (**C**), and NIH 3T3 (**D**). Cells were treated as indicated – based on previous determined IC_{50} of **CB**. Cells were fixed with *para*formaldehyde and stained for F-actin using fluorescently coupled phalloidin-ATTO488 (greyscale) and for nuclear DNA using DAPI (pseudo colored in blue). Multinucleated cells upon **BQTML-CB** treatment are highlighted by orange arrowheads. F-actin accumulations at the periphery of Rat2 wells are indicated by green arrowheads. Representative scale bars in respective DMSO images corresponds to 25 nm.

Staining revealed high numbers of multinucleated cells co-occurring with enlarged cell size, diminished lamellipodia - F-actin rich structures at the cell periphery considered as hallmarks of protrusion – and a largely intact stress fiber network – contractile, anti-parallel F-actin bundles - in U-2OS cells upon **BQTML-CB** treatment. These effects were comparable to **CB** low and high dose treatments (Figure 5A). Similar cellular effects were found for NIH 3T3 cells, but lacking cell size enlargement. This effect was rather reminiscent of **CB** low than high dose treatment, as the latter features a strongly disrupted actin filament network next to multinucleation (Figure 5D). In contrast, multinucleation induced by **BQTML-CB** treatment in Rat2 cells appeared weakened. Actin staining showed a largely intact actin network, but a striking increase of peripheral F-actin accumulations probably representing membrane ruffles compared to DMSO control.

However, **CB** treatment induced extensive and enlarged multinucleated cells at low concentrations that is conjoined with massive actin disruption at higher concentrations (Figure 5C). The impact of **BQTML-CB** in B16-F1 cells was mostly indiscernible from the DMSO control with only mild effects on the general cell viability manifesting in less but still pronounced lamellipodial structures, whereas both **CB** low and high dose concentrations led to multinucleation and highly reorganized actin structures (Figure 5B). Based on these results, it is quite likely that the potential release of **CB** induced the highlighted cellular effects – multinucleation, cell size enlargement, and actin reorganization in U-2OS, NIH 3T3 and Rat2 – and was causative for impaired cell proliferation.

Finally, to settle if the cellular effects on actin were provoked by cleaved **CB** or even by **BQTML-CB** itself, we strived to re-extract the compounds from spiked growth media subsequent to cell treatment as recently described.[66]

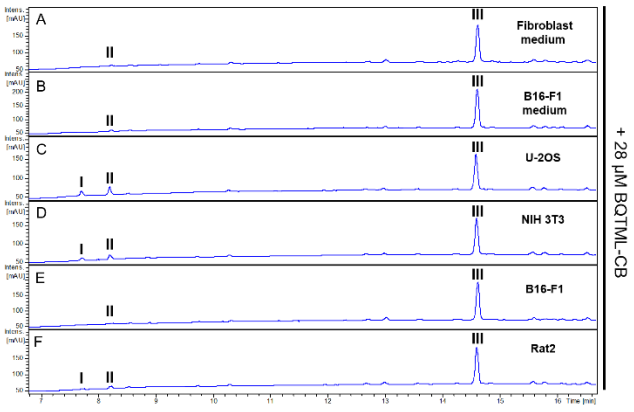

Figure 6. HPLC-MS UV chromatograms of re-extractions experiments at 210 nm. Fibroblast and B16-F1 medium were supplemented with 28 µM **BQTML-CB** and supplied to U-2OS (**C**), NIH 3T3 (**D**), B16-F1 (**E**), and rat2 (**F**) or sustained in a cell-free environment as controls for 3 h under cell culture conditions. Re-extractions were performed from removed media using 2 mL EtOAc and extracts were measured by HPLC-MS. Distinct peaks correspond to **BQTML**-derived hydrobenzoquinone **HBQ** (I), **CB** (II), and **BQTML-CB** (III) identified by respective mass spectra (see Figure S2 in the Supporting Information).

No-treatment controls were used to exclude instability and decomposition of **BQTML-CB** to **CB** over time in standard cell culture medium. Finally, two peaks were identified to correspond to **BQTML-CB** (711 Da, RT = 8.25 min, III) and **CB** (479 Da, RT = 14.5 min, II) in all extracts and a minor peak in extracts C, D and F potentially representing the cleaved **HBQ** (236 Da, RT = 7.75 min, I; Figure 6). Extracts of medium controls (A+B) and B16-F1 (E) showed scarce amounts of **CB**, probably representing impurities derived from preparative purification steps, whereas extracts derived from treatments of U-2OS (C), NIH 3T3 (D), and Rat2 (F) cells contained the cleaved **HBQ**. Summarizing, we confirmed the conversion of **BQTML-CB** to **CB** and **HBQ** in the presence of U-2OS, NIH 3T3 and – to a somewhat lesser extent – in Rat2 cells, whereas **BQTML-CB** remained stable during exposure of B16-F1 cells. This nicely corroborates our observations derived from staining experiments, which can now be correlated with cleavage of **BQTML-CB**. Actin reorganization, multinucleation and cellular enlargement are well-documented hallmarks of **CB** bioactivity that is linked to the inhibition of F-actin and the F-actin containing contractile ring, ultimately disturbing cytokinesis,[76,77] and impairing proliferative capabilities, as especially shown for U-2OS cells over the course of this study. NQO1 expression have been reported to differ across the surveyed cell lines, with U-2OS cell lines showing ample levels, while B16-F1 cells were reported virtually devoid of NQO1 expression. This fits well with less dramatic NIH 3T3 and Rat2 cell enlargements and impairment of proliferation upon **BQTML-CB** treatment mentioned above, best explained by a potentially lower, and no conversion of **BQTML-CB** to **CB** in B16-F1 cells. Here, B16-F1 turned out to be the only cell line lacking any conversion of **BQTML-CB** to **CB**, which nicely fits to the literature, describing B16-F1 as NQO1 non-expressing cell line.[70] However, a quantification of NQO1 expression in these cell lines still have to be done in the future.

Conclusion

In summary, we successfully converted the potent cytostatic cytochalasin B (**CB**) into the NQO1-resposive prodrug **BQTML-CB**. **BQTML-CB** was generated by semi-synthesis in an efficient three-step sequence, starting with **CB** obtained from the endophytic fungus *Preussia similis* G22 (DSM 32328). Here, we demonstrated the enzymatic cleavage of **BQTML-CB** to **CB** and **HBQ** *in vitro* in the presence of human NQO1. In addition, we identified one non-responding (B16-F1) and three **BQTML-CB** responding cell lines – namely U-2OS, NIH 3T3 and Rat2 – able to split **BQTML-CB** and yield the active actin inhibitor **CB** and its side product **HBQ**. Our results clearly demonstrated that NQO1 activated **CB** caused dramatic effects on cell proliferation accompanied by typical characteristics of disturbed cytokinesis induced by **CB** such as multinucleation, cell enlargement and actin disruption, with most prominent effects observed for the osteosarcoma-derived cell line U-2OS. As NQO1 is described to be overexpressed in cancer cell lines compared to healthy tissues,[78] we nicely confirmed that proliferation of non-cancer cells, such as the herein tested NIH 3T3 and Rat2 (both fibroblasts), was not significantly affected by the compound

despite their capability to process **BQTML-CB** to small degrees. Thus, our novel developed prodrug **BQTML-CB** turned out to be an interesting cancer-related migrastatic with distinct activities on cancer cell proliferation and – according to first preliminary data (not shown) - promising activity on migration. To test the applicability of the compound in a real-world scenario, we co-cultured the **BQTML-CB** responding U-2OS with non-responding B16-F1 cells (see Figure S1 in the Supporting Information). This led to astonishing effects on the actin network in B16-F1 cells comparable to **CB** treatments as shown in Figure 5. **CB** is well known to be membrane permeable, and it is hence likely to assume that the cleaved and activated **CB** can diffuse into surrounding cells and affect even NQO1-deficient cells like B16-F1. Considering the high cellular heterogeneity of tumors,[79] these bystander effects[80,81] might be beneficial to a certain extent to prevent tumor migration. However, to improve the selectivity of cytochalasan-based prodrugs for the targeted cancer cells one way might be to modify the prodrug in a way that the cargo remains inside the cell post-cleavage. Beneath manipulation of membrane permeability, cytochalasans reported as being irreversible, such as deoxaphomin[82] and pseudofuscochalasin A[83] would represent further interesting candidates for **BQTML** coupling. However, the precise molecular mechanism behind their irreversibility on actin organization is still subject of ongoing investigations.[22] Finally, we conclude that modification of the C7-OH position, as is the case for **BQTML-CB**, to generate tumor-targeted prodrugs indeed represents a suitable strategy to harness the migrastatic activity of cytochalasans such as **CB**.

Supporting Information

The authors have cited additional references within the Supporting Information.[66,75,84–86]

Acknowledgements

We gratefully acknowledge the German Research Foundation (DFG) for research funding through the CytoLabs consortium (DFG Research Unit FOR 5170). We are also thankful to the Swedish NMR Center (SNC, GU) and the Proteomics Core Facility (PFC, GU) for analytical support. The content of this work is solely the responsibility of the authors and does not necessarily represent the official views of the funding agencies.

[1] H. Sung, J. Ferlay, R. L. Siegel, M. Laversanne, I. Soerjomataram, A. Jemal, F. Bray, *CA. Cancer J. Clin.* **2021**, *71*, 209–249.
[2] J. Prick, G. de Haan, A. R. Green, D. G. Kent, *Exp. Hematol.* **2014**, *42*, 841–851.
[3] P. C. Nowell, *Science* **1976**, *194*, 23–28.
[4] H. Dillekås, M. S. Rogers, O. Straume, *Cancer Med.* **2019**, *8*, 5574–5576.
[5] J. Fares, M. Y. Fares, H. H. Khachfe, H. A. Salhab, Y. Fares, *Signal Transduct. Target. Ther.* **2020**, *5*, 28.
[6] A. Gandalovičová, D. Rosel, M. Fernandes, P. Veselý, P. Heneberg, V. Čermák, L. Petruželka, S. Kumar, V. Sanz-Moreno, J. Brábek, *Trends in Cancer* **2017**, *3*, 391–406.
[7] D. Rosel, M. Fernandes, V. Sanz-Moreno, J. Brábek, *Trends in Cancer* **2019**, *5*, 755–756.
[8] S. Gayan, S. Doshi, T. Dey, in *Handb. Oxidative Stress Cancer Ther. Asp.*, Springer Nature Singapore, Singapore, **2022**, pp. 3157–3179.
[9] M. Trendowski, *Biochim. Biophys. Acta - Rev. Cancer* **2014**, *1846*, 599–616.
[10] M. Trendowski, T. D. Christen, C. Acquafondata, T. P. Fondy, *BMC Cancer* **2015**, *15*, 632.
[11] M. Raudenská, K. Petrláková, T. Juriňáková, J. Leischner Fialová, M. Fojtů, M. Jakubek, D. Rösel, J. Brábek, M. Masařík, *Trends in Cancer* **2023**, *9*, 293–308.
[12] A. Gandalovičová, D. Rosel, J. Brábek, in *Approaching Complex Dis. Hum. Perspect. Heal. Sci. Technol. 2* (Ed.: M. Bizzarri), **2020**, pp. 203–211.
[13] K. Rottner, J. Faix, S. Bogdan, S. Linder, E. Kerkhoff, *J. Cell Sci.* **2017**, *130*, 3427–3435.
[14] M. Binder, C. Tamm, *Angew. Chem. Int. Ed.* **1973**, *12*, 370–380.
[15] C. Chepkirui, M. Stadler, *Mycol. Prog.* **2017**, *16*, 477–494.
[16] M. Stadler, J. Fournier, D. N. Quang, A. Y. Akulov, *Nat. Prod. Commun.* **2007**, *2*, 1934578X0700200.
[17] E. Skellam, *Nat. Prod. Rep.* **2017**, *34*, 1252–1263.
[18] K. Scherlach, D. Boettger, N. Remme, C. Hertweck, *Nat. Prod. Rep.* **2010**, *27*, 869–886.
[19] S. Bräse, A. Encinas, J. Keck, C. F. Nising, *Chem. Rev.* **2009**, *109*, 3903–3990.
[20] K. T. Yuyama, L. Wendt, F. Surup, R. Kretz, C. Chepkirui, K. Wittstein, C. Boonlarppradab, S. Wongkanoun, J. Luangsa-ard, M. Stadler, W.-R. Abraham, *Biomolecules* **2018**, *8*, 129.
[21] R. Kretz, L. Wendt, S. Wongkanoun, J. Luangsa-ard, F. Surup, S. Helaly, S. Noumeur, M. Stadler, T. Stradal, *Biomolecules* **2019**, *9*, 73.
[22] C. Lambert, K. Schmidt, M. Karger, M. Stadler, T. E. B. Stradal, K. Rottner, *Biomolecules* **2023**, *13*, 1247.
[23] M. Sellstedt, M. Schwalfenberg, S. Ziegler, A. P. Antonchick, H. Waldmann, *Org. Biomol. Chem.* **2015**, *14*, 50–54.
[24] B. Formánek, D. Dupommier, T. Volfová, S. Rimpelová, A. Škarková, J. Herciková, D. Rösel, J. Brábek, P. Perlíková, *RSC Med. Chem.* **2023**, *15*, 322–343.
[25] M. Binder, C. Tamm, W. B. Turner, H. Minato, *J. Chem. Soc. Perkin Trans. 1* **1973**, 1146.
[26] M. Trendowski, *Anticancer. Agents Med. Chem.* **2015**, *15*, 327–335.
[27] P. F. Bousquet, L. A. Paulsen, C. Fondy, K. M. Lipski, K. J. Loucy, T. P. Fondy, *Cancer Res.* **1990**, *50*, 1431–9.
[28] M. R. Steiner, B. Altenburg, C. S. Richards, J. P. Dudley, D. Medina, J. S. Butel, *Cancer Res.* **1978**, *38*, 2719–21.
[29] D. Medina, C. J. Oborn, B. B. Asch, *Cancer Res.* **1980**, *40*, 329–33.
[30] D. Bogyo, S. R. E. Fondy, L. Finster, C. Fondy, S. Patil, T. P. Fondy, *Cancer Immunol. Immunother.* **1991**, *32*, 400–405.
[31] M. Trendowski, J. M. Mitchell, C. M. Corsette, C. Acquafondata, T. P. Fondy, *Invest. New Drugs* **2015**, *33*, 290–299.
[32] J. Singh, R. D. Hood, *Teratology* **1987**, *35*, 87–93.
[33] K. Kapoor, J. S. Finer-Moore, B. P. Pedersen, L. Caboni, A. Waight, R. C. Hillig, P. Bringmann, I. Heisler, T. Müller, H. Siebeneicher, R. M. Stroud, *Proc. Natl. Acad. Sci.* **2016**, *113*, 4711–4716.
[34] S. H. Zigmond, J. G. Hirsch, *Science* **1972**, *176*, 1432–1434.
[35] C. Y. Jung, A. L. Rampal, *J. Biol. Chem.* **1977**, *252*, 5456–5463.
[36] A. L. Rampal, H. B. Pinkofsky, C. Y. Jung, *Biochemistry* **1980**, *19*, 679–683.
[37] H. B. Pinkofsky, D. S. Dwyer, R. J. Bradley, *Life Sci.* **1999**, *66*, 271–278.
[38] E. S. Reckzeh, H. Waldmann, *ChemBioChem* **2020**, *21*, 45–52.
[39] G. Stork, Y. Nakahara, Y. Nakahara, W. J. Greenlee, *J. Am. Chem. Soc.* **1978**, *100*, 7775–7777.
[40] G. Stork, E. Nakamura, *J. Am. Chem. Soc.* **1983**, *105*, 5510–5512.
[41] A. M. Haidle, A. G. Myers, *Proc. Natl. Acad. Sci. U. S. A.* **2004**, *101*, 12048–12053.
[42] C. Tian, X. Lei, Y. Wang, Z. Dong, G. Liu, Y. Tang, *Angew. Chem. Int. Ed.* **2016**, *128*, 7106–7110.
[43] H. Dyke, P. G. Steel, E. J. Thomas, *J. Chem. Soc. Perkin Trans. 1* **1989**, 525.
[44] B. M. Trost, M. Ohmori, S. A. Boyd, H. Okawara, S. J. Brickner, *J. Am. Chem. Soc.* **1989**, *111*, 8281–8284.
[45] E. Vedejs, J. G. Reid, *J. Am. Chem. Soc.* **1984**, *106*, 4617–4618.
[46] E. Vedejs, J. D. Rodgers, S. J. Wittenberger, *J. Am. Chem. Soc.* **1988**, *110*, 4822–4823.
[47] K. S. Yeung, I. Paterson, *Angew. Chem. Int. Ed.* **2002**, *41*, 4632–4653.
[48] M. Zaghouani, O. Gayraud, V. Jactel, S. Prévost, A. Dezaire, M. Sabbah, A. Escargueil, T. L. Lai, C. Le Clainche, N. Rocques, S. Romero, A. Gautreau, F. Blanchard, G. Frison, B. Nay, *Chem. Eur. J.* **2018**, *24*, 16686–16691.
[49] E. J. Thomas, J. W. F. Whitehead, *J. Chem. Soc., Chem. Commun.* **1986**, 727–728.
[50] E. Merifield, E. J. Thomas, *J.Chem.Soc., Chem. Commun.* **1990**, 464–466.
[51] M. Zaghouani, C. Kunz, L. Guédon, F. Blanchard, B. Nay, *Chem. Eur. J.* **2016**, *22*, 15257–15260.
[52] S. M. Canham, L. E. Overman, P. S. Tanis, *Tetrahedron* **2011**, *67*, 9837–9843.
[53] J. Reyes, N. Winter, L. Spessert, D. Trauner, *Angew. Chem. Int. Ed.* **2018**, *57*, 15587–15591.
[54] D. Lücke, Y. Linne, K. Hempel, M. Kalesse, *Org. Lett.* **2018**, *20*, 4475–4477.
[55] E. Merifield, E. J. Thomas, *J. Chem. Soc. Perkin Trans. 1* **1999**, 3269–3283.

[56] X. Long, Y. Ding, H. Wu, J. Deng, *Synlett* **2020**, *31*, 301–308.
[57] H. Dyke, R. Sauter, P. Steel, E. J. Thomas, *J. Chem. Soc. Chem. Commun.* **1986**, 1447–1449.
[58] Y. Y.-L. Zhao, X.-W. X. Long, H. Wu, J. Deng, *Org. Chem. Front.* **2022**, *9*, 6979–6998.
[59] H. Zhang, J. Zhang, R. Bao, C. Tian, Y. Tang, *Tetrahedron Chem* **2022**, *2*, 100022.
[60] H. Zhu, C. Chen, Q. Tong, Y. Zhou, Y. Ye, L. Gu, Y. Zhang, in *J. Am. Chem. Soc.*, **2021**, pp. 1–134.
[61] K. Speck, T. Magauer, *Beilstein J. Org. Chem.* **2013**, *9*, 2048–2078.
[62] C. Lambert, L. Shao, H. Zeng, F. Surup, P. Saetang, M. C. Aime, D. R. Husbands, K. Rottner, T. E. B. Stradal, M. Stadler, *Mycologia* **2023**, *115*, 277–287.
[63] B. M. Kemkuignou, C. Lambert, K. Schmidt, L. Schweizer, E. G. M. Anoumedem, S. F. Kouam, M. Stadler, T. Stradal, Y. Marin-Felix, *Fitoterapia* **2023**, *166*, 105434.
[64] C. Wang, C. Lambert, M. Hauser, A. Deuschmann, C. Zeilinger, K. Rottner, T. E. B. Stradal, M. Stadler, E. J. Skellam, R. J. Cox, *Chem. – A Eur. J.* **2020**, *26*, 13578–13583.
[65] C. Wang, V. Hantke, R. J. Cox, E. Skellam, *Org. Lett.* **2019**, *21*, 4163–4167.
[66] M. D. Kagho, K. Schmidt, C. Lambert, T. Kaufmann, J. Faix, K. Rottner, M. Stadler, T. Stradal, P. Klahn, *ChemRxiv* **2024**, DOI: 10.26434/chemrxiv-2024-qlj57.
[67] U. B. Nair, P. B. Joel, Q. Wan, S. Lowey, M. A. Rould, K. M. Trybus, *J. Mol. Biol.* **2008**, *384*, 848–864.
[68] R. V. Nair, S. Zhao, E. Terriac, F. Lautenschläger, J. H. R. Hetmanski, P. T. Caswell, A. del Campo, *ChemRxiv* **2020**, DOI: 10.26434/chemrxiv.12609545.v1.
[69] O. A. Okoh, P. Klahn, *ChemBioChem* **2018**, *19*, 1668–1694.
[70] X. Li, Z. Liu, A. Zhang, C. Han, A. Shen, L. Jiang, D. A. Boothman, J. Qiao, Y. Wang, X. Huang, Y.-X. Fu, *Nat. Commun.* **2019**, *10*, 3251.
[71] K. Zhang, D. Chen, K. Ma, X. Wu, H. Hao, S. Jiang, *J. Med. Chem.* **2018**, *61*, 6983–7003.
[72] Z. Cheng, W. O. Valença, G. G. Dias, J. Scott, N. D. Barth, F. de Moliner, G. B. P. Souza, R. J. Mellanby, M. Vendrell, E. N. da Silva Júnior, *Bioorg. Med. Chem.* **2019**, *27*, 3938–3946.
[73] H. Asgharian, L. Chen, L. Fish, A. Navickas, J. Yu, B. Woo, A. S. Nanda, B. Choi, S. Zhou, J. Rabinowitz, H. Goodarzi, *Nat. Cancer* **2023**, *4*, 682–698.
[74] X. Wang, Y. Liu, A. Han, C. Tang, R. Xu, L. Feng, Y. Yang, L. Chen, Z. Lin, *Oncogene* **2022**, *41*, 5107–5120.
[75] R. D. Rohde, H. D. Agnew, W. S. Yeo, R. C. Bailey, J. R. Heath, *J. Am. Chem. Soc.* **2006**, *128*, 9518–9525.
[76] T. E. Schroeder, *Zeitschrift für Zellforsch. und Mikroskopische Anat.* **1970**, *109*, 431–449.
[77] J. A. Spudich, S. Lin, *Proc. Natl. Acad. Sci.* **1972**, *69*, 442–446.
[78] S. R. Punganuru, H. R. Madala, V. Arutla, R. Zhang, K. S. Srivenugopal, *Sci. Rep.* **2019**, *9*, 8577.
[79] I. Dagogo-Jack, A. T. Shaw, *Nat. Rev. Clin. Oncol.* **2018**, *15*, 81–94.
[80] F. Giugliano, C. Corti, P. Tarantino, F. Michelini, G. Curigliano, *Curr. Oncol. Rep.* **2022**, *24*, 809–817.
[81] B. Menezes, J. J. Linderman, G. M. Thurber, *Drug Metab. Dispos.* **2022**, *50*, 8–16.
[82] R. Kretz, L. Wendt, S. Wongkanoun, J. J. Luangsa-ard, F. Surup, S. E. Helaly, S. R. Noumeur, M. Stadler, T. E. B. Stradal, *Biomolecules* **2019**, *9*, 73.
[83] C. Lambert, M. J. Pourmoghaddam, M. Cedeño-Sanchez, F. Surup, S. A. Khodaparast, I. Krisai-Greilhuber, H. Voglmayr, T. E. B. Stradal, M. Stadler, *J. Fungi* **2021**, *7*, 131.
[84] N. Branda, *JoVE Sci. Educ. Database. Org. Chem.* **2019**.
[85] W. C. Still, M. Kahn, A. Mitra, *J. Org. Chem.* **1978**, *43*, 2923–2925.
[86] C. C. Jimidar, C. S. G. Ganskow, M. D. Kagho, A. Chakrabarti, M. Zollo, U. Beutling, M. Brönstrup, S. A. Sieber, S. M. Hacker, P. Klahn, *ChemRxiv* **2024**, DOI: 10.26434/chemrxiv-2024-f8x8z.

Entry for the Table of Contents

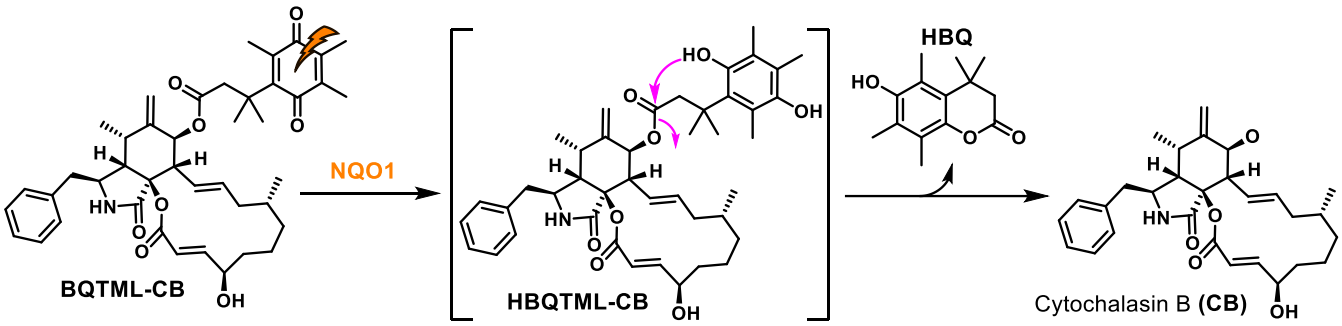

The design, synthesis and evaluation of the NQO1-targeted prodrug **BQTML-CB** is reported, representing a novel approach to improve cancer selectivity of cytochalasan-based migrastatics.

Institute and/or researcher X.com usernames: @DocKlahn, @OMC_GU, @naturvetenskap, @goteborgsuni, @helmholtz_HZI, @d_kagho, @StradalT, @RottnerKlemens, @MS_fungi